25th ABCM International Congress of Mechanical Engineering
October 20-25, 2019, Uberlândia, MG, Brazil

ANALYSIS OF VIBRATION ATTENUATION IN A BEAM COUPLED WITH A PIEZOELECTRIC IN SHUNT CONFIGURATION USING THE SPECTRAL ELEMENT METHOD

Braion Barbosa de Moura
Marcela Rodrigues Machado
University of Brasilia, Technology Faculty - Department of Mechanical Engineering.
braionmoura@hotmail.com
marcelam@unb.br

Abstract. *The study describes an analysis of the periodic, shunt piezoelectric patches applied to the attenuation of wave propagation in a beam with periodic characteristics, using the Spectral Element Method (SEM) as formulation. The Spectral Element method is used to model vibrations and monitoring applications in structural integrity, in this case addressing the coupling of a piezoelectric derivative connected to a Timoshenko beam. The approach on the subject refers to the description of several characteristics involved, such as the geometric analysis of coupling and its interactions to the behaviour in the structure, properties of metamaterials in vibrations and shunts configurations for wave attenuations. The results of this study express a structural attenuation proportional to the use of a piezoelectric shunt configuration as an actuator. The frequency response function confirms an attenuation to a frequency resonance designed for the pzt-shunt.*

Keywords: *Attenuation Frequency Ranges, Multi-Resonance Shunts, Piezoelectric Actuator, Spectral Element Method.*

1. INTRODUCTION

Metamaterials in engineering products has increased in the last few years due to the improvement of the machines as 3D printers and the manufacturing process of those materials. The inclusion of electronic sensors, e.g. piezoelectric sensor, into the structure allowed us to monitor and control the vibration in of such systems. The application of the pzts-sensors in metamaterial means the control and attenuations in wave propagation or structural camouflage. Several studies address the use of piezoelectric for vibration control and control of waves propagation in periodic rods. However, the experiments involving these studies are built on joints of the symmetrical parts of materials with various piezoelectric, which in practice causes an interference proportional to the number of parts of the element. Based on this idea, this study aims the application of metamaterial based on piezoelectric sensors (Thorp, Ruzzeneand Baz, 2001).

Several studies have addressed the uses of piezoelectric vibration control devices through passive and active techniques, as they can transform the energy from mechanical vibrations into electrical energy, which can be passively dissipated into a dissipative type electrical circuit called shunt. The numerical model that will be addressed in this paper is the Spectral Element Method (SEM).

According to Doyler (1997), the SEM describes the dynamic behaviour of an elemental model about nodal displacements in the frequency domain. Because its solution is exactly the structure can be modelled by only an element as long as it does not have any discontinuity along with the geometry under consideration. Thus, the spectral element method consists of solving the differential equations of equilibrium for periodic structures written in the frequency domain. One of its advantages in use SEM is that the amount of elements needed to represent a structure is equal to the number of its discontinuities.

This study proposes the realization of a wave propagation control in a beam with a coupled piezoelectric (PZT), using the Spectral Element Method (SEM). The objective is to estimate a relationship between the generated responses of the beam, the beam with the PZT coupling and the beam with the shunted PZT coupling. The numerical results are compared with a simple beam FRF response.

2. DERIVATION OF THE EQUATIONS OF MOTION

2.1. Formulation of the coupled equations of motion

The coupling structure of the beam with PZT was based on the study presented by Usik and Joohong (1999). The of the pzt-beam geometry is shown in Figure 1.

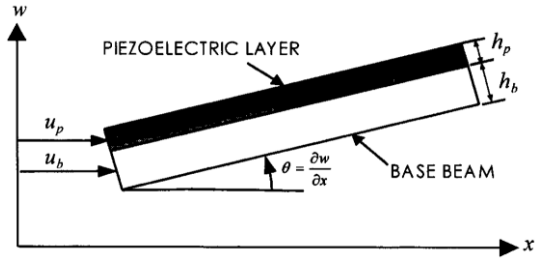

Figure 1. Geometry and deformation of the elastic-piezoelectric two-layer beam.
Fonte:(L. Usik and K. Joohong, 1999).

According to Usik and Joohong (1999), the structural dynamic equations of motion are derived considering that beam density and thickness are uniforms, the shear deformations in both layers are insignificant, and the rotational inertia has no influence. It is also adopted that the transverse displacement $w(x,t)$ is the same for both layers and the applied voltage is uniform along the beam. There is a perfect continuity in the coupling interactions, which does not slip in the interface, relying on the understanding that the linear elasticity and piezoelectricity theories are applicable.

For perfect boundary conditions, the geometry of Fig. 1 provides the kinematics relation as:

$$u_p = u_b - \frac{h_b + h_p}{2}\theta \tag{1}$$

where u_p and u_b are the axial displacement of the neutral axes of the base beam and the piezoelectric layer, respectively. Already h_b and h_p are the thickness of base the beam and the thickness of the piezoelectric layer, respectively, and $\theta = \partial\omega/\partial x$ is rotational angle of the base beam. The electromechanical model of the base beam witch a surface-mounted piezoelectric patch is based on the stress-charge form of the constitutive equations for a piezoelectric material (Standards Committee of the IEEE Ultrasonic and Frequency Control Society, 1988):

$$\begin{Bmatrix}\sigma \\ E\end{Bmatrix} = \begin{bmatrix} C_{11}^D & -h_{31} \\ -h_{31} & \beta_{33}^S \end{bmatrix} \begin{Bmatrix}\epsilon \\ D\end{Bmatrix} \tag{2}$$

where σ is the mechanical stress, ϵ the mechanical strain, D is the electrical displacement (charge/area in the beam vertical direction) and E is the electrical field (voltage/length along the vertical direction). C_{11}^D is the elastic stiffness, $\beta_{33}^S$is the dielectric constant, and h_{31} is the piezoelectric constant.

The elementary beam model supports two movements, that is, the transverse displacements $\hat{v}$ and the rotation of the cross section ϕ, where the rotation is derived from the transverse deformation as $\phi = \partial\hat{v}/\partial x$. As the changes in the beam are of shear $\hat{V}$ and bending moment $\hat{M}$, which can also be expressed in terms of transverse spectral displacement (DOYLER, 1988).

$$\frac{\partial^2\hat{v}}{\partial x^2} = EI\hat{v}''(x), \qquad \hat{V} = -EI\frac{\partial^3\hat{v}}{\partial x^3} = -EI\hat{v}'''(x) \tag{3}$$

where EI is flexural stiffness. Thus, the equation describing the dynamic motion of the beam vibration is written as:

$$\frac{EI\partial^4 v(x,t)}{\partial x^4} + \rho A(x)\frac{\partial^2 v}{\partial t^2}(x,t) = q(x,t) \tag{4}$$

The nodal displacements $\hat{v}$ and ϕ, and the nodal forces present in the beam of length L result in two nodes with two degrees of freedom and two nodal loads at each node. Since the coupling of PZT in the beam is similar to a beam geometry, we can associate the same displacements to the entire system, as shown in Figure 2.

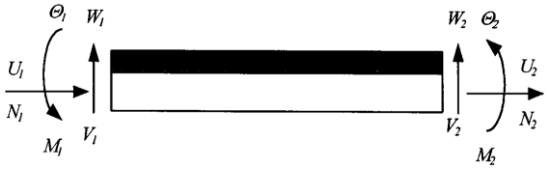

Figure 2. Sign convention for the spectral element.
Fonte:(L. Usik and K. Joohong, 1999).

Then, using the constitutive relation (2) and assuming that D is constant through the thickness of the thin piezoelectric layer, the strain energy of the two-layer beam is derived after integrating over z and assuming $E = zw''$ as

$$V = \frac{1}{2}\int_0^L \left(E_b A_b u_b'^2 + E_b I_b W''^2 + C_{11}^D A_p u_p'^2 + C_{11}^D I_p w''^2 - 2A_p h_{31} D u_p' + A_p \beta_{33}^S D^2\right) dx \tag{5}$$

where E, A, I and ρ (for each layer) are the Young's modulus, the cross-sectional area, the area moment of inertia about the neutral axis, and the mass density, respectively. The kinetic energy of the two-layer beam is also derived as

$$T = \frac{1}{2}\int_0^L \left\{\rho_b A_b (\dot{u}_b^2 + \dot{w}^2) + \rho_p A_p \left(\dot{u}_p^2 + \dot{w}^2\right)\right\} dx \tag{6}$$

The virtual work is given by

$$\delta W = \int_0^L bV(t)\delta D dx + \bar{N}\delta u_b \,|_L^0 + \bar{M}\delta\theta \,|_L^0 + \bar{Q}\delta w \,|_L^0 \tag{7}$$

In the above equations, the prime ($'$) and the dot ($\cdot$) indicate the particular derivates witch respect to the coordinate x and the time t, respectively. $V(t)$ is the applied voltage. The axial displacement of the piezoelectric layer up can be eliminated from two energy expressions, Eqs. (5) and (6), by using Eq. (1). Applying these energies into Hamilton's principle yields the axial-bending coupled equations of motion as

$$\begin{aligned} &EIw''' + \rho A\ddot{w} = -\alpha\ddot{u}'_b + \beta u_b''' + \gamma\ddot{w}'' \\ &EIu_b'' - \rho A\ddot{u}_b = -\alpha\ddot{w}' + \beta w''' \end{aligned} \tag{8}$$

where,

$$\begin{aligned} &\rho A = \rho_b A_b + \rho_p A_p, \qquad EA = E_b A_b + E_p A_p, \qquad EI = E_b I_b + C_{11}^D I_p + \frac{1}{4}E_p A_p h^2 \\ &\alpha = \frac{1}{2}\rho_p A_p h, \qquad \beta = \frac{1}{2}E_p A_p h, \qquad \gamma = \frac{1}{4}\rho_p A_p h^2 \\ &h = h_b + h_p, \qquad E_p = C_{11}^D - \frac{h_{31}^2}{\beta_{33}^S} \end{aligned} \tag{9}$$

In Eq. (8), α and β are the parameters that govern the axial-bending coupling. Without the piezoelectric constraining layer, the parameters α, β, and γ will vanish to result in two independent de-coupled equations of motion for the pure-bending motion and the pure axial-motion of the base beam. The Hamilton principle also provides the boundary conditions related to the mechanical and piezoelectric variable as

$$\begin{aligned} &N = \bar{N} \;\; or \;\; u_b = \overline{u_b} = EAu_b' - \beta w'' - bd_{31}E_p V(t) \\ &M = \bar{M} \;\; or \;\; \theta = \bar{\theta} = EIw'' - \beta u_b' + \frac{1}{2}hbd_{31}E_p V(t) \\ &Q = \bar{Q} \;\; or \;\; w = \overline{w} = -EIw''' - \alpha\ddot{u}_b'' - \gamma\ddot{w}' \end{aligned} \tag{10}$$

The over-bar in Eq. (11) indicates the quantities specified at boundaries. Where d_{31} is the piezoelectric constant defined by $d_{31} = h_{31}/(E_p\beta_{33}^S)$, and N, M, and Q are the resultant axial force, resultant bending moment, and the resultant bending moment, and the resultant transverse shear force Q, respectively. The governing equations of motion for the elastic-elastic two-layer beam can be readily reduced from the above formulations by merely eliminating all piezoelectric terms. A similar formulation was given by Liao (1997), but his work was for the cantilevered beam that is partially laminated with a piezoelectric patch.

2.2 Spectral element analysis

According to Usik and Joohong., (1999), the spectral element will be formulated from the general solutions of Eq. (8). Assume that the dynamic responses of the beam and the applied voltage have the spectral representations as

$$\begin{aligned} w(x,t) &= \sum_{n}^{N} \widehat{W}(x,\omega_n) e^{i\omega_n t} \\ u_b(x,t) &= \sum_{n}^{N} \widehat{U}(x,\omega_n) e^{i\omega_n t} \\ V(t) &= \sum_{n}^{N} \widehat{V}(\omega_n) e^{i\omega_n t} \end{aligned} \tag{11}$$

where ω_n is the frequency and $\widehat{W}$, $\widehat{U}$ and $\widehat{V}$ are the spectral components of w, u_b, and V, respectively. N is the total number of spectral components summed in Eq. (11). Once the Nyquist frequency ω_{NF} (i.e. the maximum frequency range to be considered in the spectral analysis) is chosen, N is determined by shorthand, the summation and subscripts used in Eq. (11) will be omitted in the following.

By substituting Eq. (11) into Eq. (8) and cancelling the common time factor may yield coupled two ordinary differential equations for $\widehat{W}$ and $\widehat{U}$ as

$$\begin{aligned} EI\widehat{W}'''' - \omega^2 \rho A \widehat{W} &= \omega^2\left(-\gamma \widehat{W}'' + \alpha \widehat{U}'\right) + \beta \widehat{U}''' \\ EA\widehat{U}'' + \omega^2 \rho A \widehat{U} &= \omega^2 \alpha W' + \beta \widehat{W}'''' \end{aligned} \tag{12}$$

The general solutions for $\widehat{W}$ and $\widehat{U}$ can be obtained in the forms of

$$\begin{aligned} \widehat{W}(x) &= \sum_{i=1}^{3} \left(A_i e^{\frac{k_i x}{L}} + A_{2i} e^{-\frac{k_i x}{L}} \right) = [\boldsymbol{N}(x)]\{\boldsymbol{A}\} \\ \widehat{U}(x) &= \sum_{i=1}^{3} \left(B_i e^{\frac{k_i x}{L}} + B_{2i} e^{-\frac{k_i x}{L}} \right) = [\boldsymbol{N}(x)]\{\boldsymbol{B}\} \end{aligned} \tag{13}$$

where,

$$\begin{aligned} [\boldsymbol{N}(x)] &= [e^{\frac{k_1 x}{L}} \;\; e^{\frac{k_2 x}{L}} \;\; e^{\frac{k_3 x}{L}} \;\; e^{-\frac{k_1 x}{L}} \;\; e^{-\frac{k_2 x}{L}} \;\; e^{-\frac{k_3 x}{L}}] \\ \{\boldsymbol{A}\} &= \{A_1 \;\; A_2 \;\; A_3 \;\; A_4 \;\; A_5 \;\; A_6\} \\ \{\boldsymbol{B}\} &= \{B_1 \;\; B_2 \;\; B_3 \;\; B_4 \;\; B_5 \;\; B_6\} \end{aligned} \tag{14}$$

In Eq. (13), $k_i (i = 1, 2, 3)$ are the wave numbers to be computed from,

$$(\beta^2 - EAEI)k^6 + \omega^2 L^2 (2\alpha\beta - \rho AEI - \gamma EA)k^4 + \omega^2 L^4 (\alpha^2 \omega^4 + \rho A(EA - \gamma\omega^2)\}k^2 \; + \omega^4 L^6 \rho A^2 = 0 \tag{15}$$

Equations (15) is the dispersion relation that gives the relation between wave number and frequency. At a specified frequency ω, it gives six values of wave number k, that is in pairs. The relations between the coefficients A_i and B_i of Eq. (13) can be obtained by substituting Eq. (13) into Eq. (12) as

$$B_i = (-1)^i \left\{ \frac{L^4 \rho A \omega^2 + L^2 \gamma \omega^2 k_i^2 + EIk_i^4}{Lk_i (L^2 \alpha \omega^2 - \beta k_i^2)} \right\} A_i = \lambda_i(\omega) A_i \quad (i = 1, 2, \ldots 6) \tag{16}$$

or simply

$$\{\boldsymbol{B}\} = [diagonal(\lambda_i)]\{\boldsymbol{A}\} \tag{17}$$

By substitute Eq. (17) into Eq. (13) to express $\widehat{U}$ as the function of A_i. The coefficients A_i can be determined by applying Eq. (13) into the boundary conditions of Eq. (10). The coefficients B_i can be then computed from Eq. (17). The coupling functions $\lambda_i(x)$ in Eq. (16) indicate the existence of the coupling between the axial-motion and the bending-motion of the base beam. Infinite or zero values of $\lambda_i(x)$ simply imply the decoupling. When the piezoelectric layer thickness vanishes, it can be shown that the coefficients A_5, A_6, B_1, B_2, B_3, and B_4 indeed vanish to result in decoupled two problems: the pure bending-motion problem and the pure axial-motion problem. The spectral nodal DOF defined in Fig. 2 can be expressed in terms of A_i, by using Eq. (13), as

$$\{\boldsymbol{X}\} = [\boldsymbol{Q}]\{\boldsymbol{A}\} \tag{18}$$

where $\boldsymbol{X}$ is the spectral nodal DOF vector defined by

$$\{\boldsymbol{X}\} = \left\{\widehat{U}_1 \;\; \widehat{W}_1 \;\; \widehat{\Theta}_1 \;\; \widehat{U}_2 \;\; \widehat{W}_2 \;\; \widehat{\Theta}_2\right\}^T \tag{19}$$

Using Eqs. (17) and (18), the spectral displacement components of Eq. (13) can be represented in terms of the spectral nodal DOF vector as

$$\begin{aligned} \widehat{W}(x) &= [\boldsymbol{N}(x)][\boldsymbol{Q}]^{-1}\{\boldsymbol{X}\} \\ \widehat{U}(x) &= [\boldsymbol{N}(x)[diagonal(\lambda_i)]\{\boldsymbol{Q}\}]^{-1}\{\boldsymbol{X}\} \end{aligned} \tag{20}$$

Substituting Eq. (13) into the spectral representations of the force-displacement relations of Eq. (10), the spectral components of the nodal forces and moments defined in Fig 2 can be expressed in terms of A_i as

$$\{\boldsymbol{f}\} = [\boldsymbol{P}]\{\mathbf{A}\} \tag{21}$$

where,

$$\{\boldsymbol{f}\} = \left[\widehat{N}_1 - \widehat{N}^e \quad \widehat{Q}_1 \quad \widehat{M}_1 + \widehat{M}^e \quad \widehat{N}_2 + \widehat{N}_2^e \quad \widehat{Q}_2 \quad \widehat{M}_2 - \widehat{M^e}\right]^T \tag{22}$$

In Eq. (22), $\widehat{N}_b, \widehat{Q}_b, \widehat{M}_i$ and are the nodal spectral components of axial force, the nodal transverse shear force and nodal bending moment defined in Fig. 2, respectively. Similarly, $\widehat{N}^e$ and $\widehat{M}^e$ are the nodal spectral components of piezoelectrically induced axial force and bending moment defined by,

$$\widehat{N}^e = bd_{31}E_p\widehat{V}, \qquad \widehat{M}^e = \frac{1}{2}hbd_{31}E_p\widehat{V} \tag{23}$$

By eliminating the coefficients A_i from Eqs. (18) and (21) yields the spectral nodal force-nodal displacement relation as

$$\{\boldsymbol{f}\} = [\boldsymbol{P}][\boldsymbol{Q}]^{-1}\{\boldsymbol{X}\} = [\boldsymbol{S}]\{\boldsymbol{X}\} \tag{24}$$

where $\boldsymbol{S}$ is the frequency-dependent spectral element matrix. Also known as a dynamic stiffness matrix, the terms of the dynamics stiffness matrix for the system are extensive and computationally expensive to obtain analytically. Explicit expression for $\boldsymbol{S}$ has become possible due to recent advance in symbolic computing (FITCH, 1985). The explicit expressions for $\boldsymbol{P}$ and $\boldsymbol{Q}$ are listed herein as

$$[\boldsymbol{P}] = \frac{1}{L^3}\begin{bmatrix} p_{11} & p_{11} & p_{12} & p_{12} & p_{13} & p_{13} \\ p_{21} & -p_{21} & p_{22} & -p_{22} & p_{23} & -p_{23} \\ p_{31} & p_{31} & p_{32} & p_{32} & p_{33} & p_{33} \\ -e^{k_1}p_{11} & -e^{-k_1}p_{11} & -e^{k_2}p_{12} & -e^{-k_2}p_{12} & -e^{k_3}p_{13} & -e^{-k_3}p_{13} \\ -e^{k_1}p_{21} & -e^{-k_1}p_{21} & -e^{k_2}p_{22} & -e^{-k_2}p_{22} & -e^{k_3}p_{23} & -e^{-k_3}p_{23} \\ -e^{k_1}p_{31} & -e^{-k_1}p_{31} & -e^{k_2}p_{32} & -e^{-k_2}p_{32} & -e^{k_3}p_{33} & -e^{-k_3}p_{33} \end{bmatrix} \tag{25}$$

$$[\boldsymbol{Q}] = \begin{bmatrix} \lambda_1 & -\lambda_1 & \lambda_2 & -\lambda_2 & \lambda_3 & -\lambda_3 \\ 1 & 1 & 1 & 1 & 1 & 1 \\ \frac{k_1}{L} & \frac{-k_1}{L} & \frac{k_2}{L} & \frac{-k_2}{L} & \frac{k_3}{L} & \frac{-k_3}{L} \\ e^{k_1}\lambda_1 & -e^{-k_1}\lambda_1 & e^{k_2}\lambda_2 & -e^{-k_2}\lambda_2 & e^{k_3}\lambda_3 & -e^{-k_3}\lambda_3 \\ e^{k_1} & e^{-k_1} & e^{k_2} & e^{-k_2} & e^{k_3} & e^{-k_3} \\ \frac{e^{k_1}k_1}{L} & \frac{-e^{-k_1}k_1}{L} & \frac{e^{k_2}k_2}{L} & \frac{-e^{-k_2}k_2}{L} & \frac{e^{k_3}k_3}{L} & \frac{-e^{-k_3}k_3}{L} \end{bmatrix} \tag{26}$$

where,

$$\begin{aligned} p_{1i} &= k_i L(\beta k_i - EAL\lambda_i) \\ p_{2i} &= L^2\omega^2\gamma k_i + EIk_i^3 - L^3\omega^2\alpha\lambda_i - L\beta k_i^2\lambda_i \\ p_{3i} &= k_i L(L\beta\lambda_i - EIk_i) \end{aligned} \tag{27}$$

2.3 Single-resonance shunt

The governing equations of the system according to the behaviour of the shunted piezo patch scheme are presented in L. Airoldi, M. Ruzzene (2011). Since the work uses the construction of a single PZT coupled to the element in its proportion, some considerable modifications are made in the exposed analytical models for shunted effect analysis. Figure 3 represents the schematic of the shunted piezo patch.

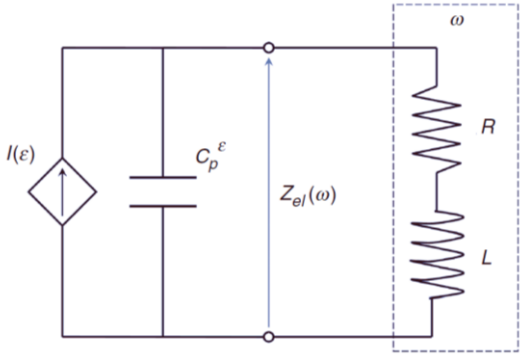

Figure 3. Equivalent circuit of the shunted piezo patch.
Fonte: (L. Airoldi, M. Ruzzene, 2011).

According to the equivalent circuit of a piezoelectric transducer, with its inherent capacitance C_p^E at constant strain, shunted through a resistor-inductor in series. The electrical admittance of the piezo patch is given by:

$$Y_{el} = Y_p + Y_{su} \tag{28}$$

where $Y_{el} = 1/Z_{el}$ introduced in the equation is the equivalent admittance of the piezo, and $Y_{el} = 1/Z_{su}$ is the admittance of the shunting circuit, with $Z_{su} = R + i\omega L$. The resulting expression of the impedance Z_{el} therefore is:

$$Z_{el}(\omega) = \frac{R + i\omega L}{\left(1 - \omega^2 LC_p^E\right) + i\omega RC_p^E} \tag{29}$$

Considering these elements involved the impedance relations, we can express the shunted influence in the matrix form:

$$[\boldsymbol{Z}] = \begin{bmatrix} N_{e1} & N_{e1} & N_{e1} & N_{e1} & N_{e1} & N_{e1} \\ 0 & 0 & 0 & 0 & 0 & 0 \\ M_{e1} & M_{e1} & M_{e1} & M_{e1} & M_{e1} & M_{e1} \\ -N_{e2} & -N_{e2} & -N_{e2} & -N_{e2} & -N_{e2} & -N_{e2} \\ 0 & 0 & 0 & 0 & 0 & 0 \\ M_{e2} & M_{e2} & M_{e2} & M_{e2} & M_{e2} & M_{e2} \end{bmatrix} \tag{30}$$

Having as its elements:

$$N_{e1} = N_{e2} = \frac{Z_t^2 i\omega Z_{ef} b d_{31} E_p}{1 + i\omega C_p Z_{ef}}$$
$$M_{e1} = M_{e2} = \frac{Z_t^2 i\omega Z_{ef} h b d_{31} E_p}{2 + 2i\omega C_p Z_{ef}} \tag{31}$$

Given these relations, we can determine the general spectral matrix of the system with the shunted configuration, as follows:

$$[\boldsymbol{S}] = [\boldsymbol{P}][\boldsymbol{Q}]^{-1} + [\boldsymbol{Z}] \tag{32}$$

3. NUMERICAL ANALYSIS

To validate the coupling attenuation models, the properties of the beam and PZT were the same as those of Usik and Joohong (1999), presented in Table 1.

Table 1. Mechanical and geometric properties of the beam and electro-mechanical properties of the piezoelectric material.

Composite Properties	Units of Measurement	Beam	Piezoelectric
Young's modulus	$[GPa]$	71.0	64.9
Density, ρ	$[kg/m^3]$	2700	7600
Length, l	$[m]$	0.2616	0.2616
Width, b	$[m]$	0.0127	0.0127
Thickness, h_b, h_p	$[m]$	0.002286	0.000762
Piezoelectric Constant, d_{31}	$[m/V \times 10^{-12}]$	-	-175
Dielectric Constant, β_{33}^S	$[m/V \times 10^{-12}]$	-	-5.6788
Elastic Stiffness, C_{11}^D	$[GPa]$	-	74.0

The high amplitude resonances collected from the divisions of the element are limited to a frequency range relative to the branch circuit. Trained some loops were chosen resistors $R_1 = 2500\ \Omega$, $R_2 = 680\ \Omega$, $R_3 = 120\ \Omega$, $R_4 = 100e^{-9}$, $R_5 = 2594\ \Omega$, inductor $L = 0.1144\ H$, capacitance $C_p^E = 200\ GPa$ and impedance $Z_t^2 = 0{,}0961$. Figure 4, represents the circuit used in the design of piezoelectric coupler in shunted.

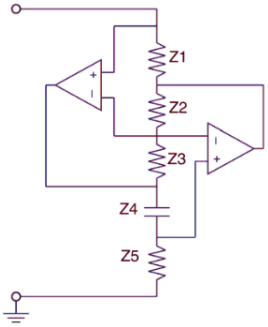

Figure 4. Sketch of the resonant circuit shunt
Fonte: (Airoldi and Ruzzene, 2011).

This association of inductors, capacitors, and other influencers can promote an impedance resonance at a frequency necessary to influence the desired structure. However, high-amplitude resonances, which are limited to a small frequency range, rely exclusively on high values of R to increase bandwidth, but reduce the overall efficiency of the electromechanical energy conversion, and hence the mechanism of attenuation. Figure 5 shows the impedance resonance, vibrating at the resonant circuit shunt desing.

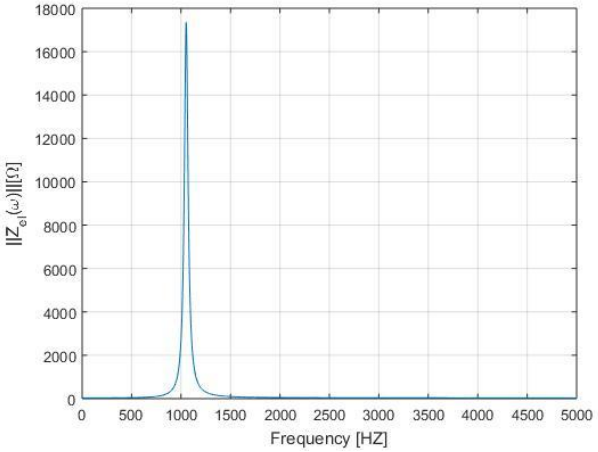

Figure 5. Frequency-dependent impedance graph considering shunt performance.

The impedance considered in Figure 5 refers to a frequency band occupancy associated with system resonance. The values to arrive at this result were adopted by speculation to coincide with a resonance of the system composed by the beam with the PZT coupled to its surface. It was considered for the coupling of the beam with the PZT, that both have the same width and the same length as shown in Table 1.

By adopting the clamped boundary condition for the system, we can expose the relationships of the beam Frequency response function (FRF) without and with the PZT coupling through Figure 7.

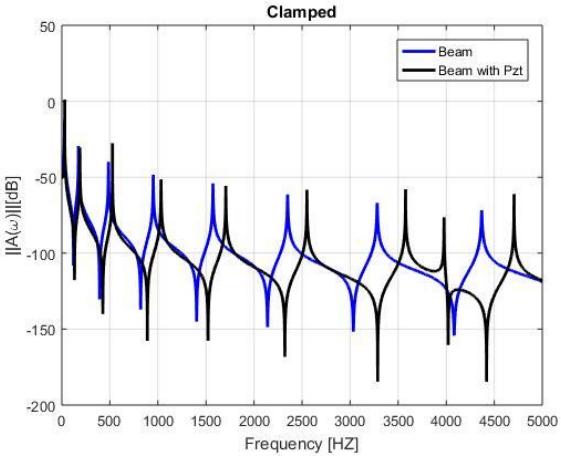

Figure 7. Frequency Response Function (FRF) of beam alone and beam with coupled PZT.

Comparing the beam responses with and without PZT, the resonance and anti-resonance peaks advance in frequency towards the PZT-coupled beam. Such a relationship is justified because the rigidity and mass of the system are changed. By imposing all conditions in the system, interpreting the adjustments of a clamped boundary condition to the impedance reported in Figure 5. The FRF of the PZT-beam coupled with the shunt configuration influenced in the system.

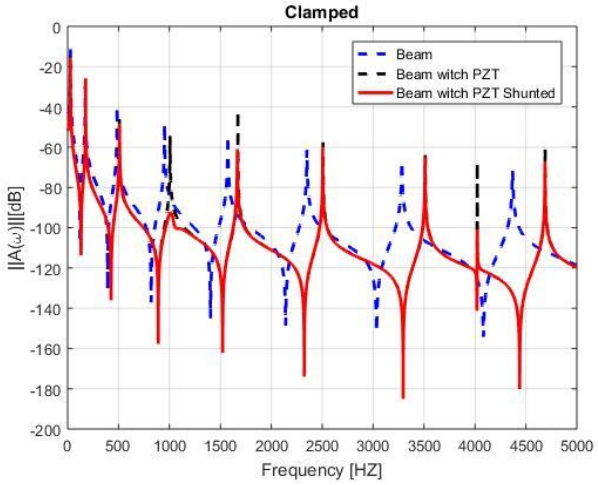

Figure 8. Frequency response function (FRF) of beam alone, beam with coupled PZT and beam witch PZT in configuration shunted.

The FRFs plotted in Figure 8 demonstrate that the PZT- beam coupled shunt configuration requires attenuation proportional to the system impedance and resonance settings. It is observed that the resonance attenuation happens at the resonance peak around 1300 Hz, same resonance frequency designed for the shunt system (see Figure 7). These relationships demonstrate that according to the shunt circuit configurations, it is possible to attenuate the oscillations of a system by using the pzts-shunt.

4. COMMENTS AND FINAL REMARKS

This paper presents a dynamic analysis of a beam system with a PZT coupling and a shunt configuration. The effects that geometric coupling provokes on oscillation are observed through FRFs, which show that the resonance peaks have changed with the associated frequencies. The impact of coupling the beam with shunted PZT demonstrated by FRF comparisons present an attenuated between 1000 Hz and 1400 Hz, same shunt impedance resonance. In other words, by analyzing and comparing the FRF of the simple beam, pzt-beam and pzt-beam shunt, we conclude that the piezoelectric association with the shunt configuration in the structure can result in vibration attenuation controls, as shown by the simulation in Figure 7.

It is estimated that the oscillatory behaviour of the system will also suffer some amplitude attenuation during propagation with piezoelectric connected in the normal formal series, in addition to the most noticeable amplitude that appears between the approximate 1400 Hz frequencies. The resonant frequency designed for the circuit shunt with resistors associated with it inductor and capactior was set to 1358 Hz. Regarding the electrical resonance impedance of the PZT branch circuit, it was observed that the effect of the resistors directly influenced Z_{el} impedance behavior and consequently influenced the attenuated frequency band.

The resonant behaviour of the considered shunt circuits, significantly affects the dynamic behaviour of the base structure, specifically around the resonant frequencies of the circuit. Such resonances can be tuned to maximize the effect of the deviation at the frequencies of interest where, in this case, the waves were attenuated where the general vibrations of the structure should be reduced. This attenuation method using shunted configurations refers to contributions to controls of various oscillatory systems arranged in a possible variance by electrical adjustments only. Thus, enabling a comprehensive solution of numerous systems for which different behaviours are desired through vibrational changes.

The paramters used in the SEM numerical model are based on estimates to improve the response of the piezoelectric association in the structure to result in a specific wave attenuation control. Next step of this work will be periodaize the structure and analyse the band gap attenuation by using a metamaterial based on the pzt-shunt, and compare the studies wiht experiment datas. .

5. REFERENCES

Doyle, J.F., 1988. A spectrally formulated finite element for longitudinal wave propagation. International Journal of Analytical and Experimental Modal Analysis.

Doyle, J.F., 1997. "Wave propagation in structure: a spectral analysis using fast discrete Fourier Transforms*", 2 nd ed. SpingerVerlag*, New York , USA.

Fitch, J., 1985. Solving algebraic problems with REDUCE. *Journal of Symbolic Computation* 1, 211±227.

L. Airoldi and M. Ruzzene. Wave Propagation Control in Beams Through Periodic Multi-Branch Shunts, *Journal of Intelligent Material Systems and Structures*, 2011.

Lee, U. (2009). Spectral Element Method in Strutural Dynamics., *Inha University Press.*

Lee, U., Lee, J., 1997. Dynamic analysis of one- and two-dimensional structures using spectral element methods. In: *Proceedings of the Sixth International Conference on Recent Advances in Structural Dynamics. ISVR*, University of Southampton.

Liao, W. H., 1997. Active-passive hybrid structural control: an enhanced active constrained layer damping treatment with edge elements. Ph.D. Thesis, The Pennsylvania State University, PA.

LI J., and Chan C. T., Double-negative acoustic metamaterial, Phys. Ver. E 70, 055602, 2004.

LIU, Z., et al., Locally Resonant Sonic Materials, Science 289, 1734, 2000.

L. Usik, K. Joohong., 1999. Dynamics of elastic-piezoelectric two-layer beams using the spectral element method. International Journal of Solids and Structures.

O. Thorp, M. Ruzzene and A. Baz, 2001. Attenuation and localization of wave propagation in rods with periodic shunted piezoelectric patches. *Institute of Physics Publishing*, 12p.

Standards Committee of the IEEE Ultrasonics, F. and U. FrequencyControl Society (1988). *IEEE standard on piezoelectricity.*

6. RESPONSIBILITY NOTICE

The authors are the only responsible for the printed material included in this paper.